

# 9

## The TL Timoshenko Plane Beam Element

## TABLE OF CONTENTS

	Page
§9.1. <b>Introduction</b>	9-3
§9.2. <b>Beam Models</b>	9-3
§9.2.1. Basic Concepts and Terminology . . . . .	9-3
§9.2.2. Mathematical Models: Classical and Timoshenko . . . . .	9-4
§9.2.3. Finite Element Models . . . . .	9-5
§9.2.4. Bernoulli-Euler versus Timoshenko Beam Elements . . . . .	9-7
§9.3. <b>X-Aligned Reference Configuration</b>	9-9
§9.3.1. Element Description . . . . .	9-9
§9.3.2. Motion . . . . .	9-9
§9.3.3. Displacement Interpolation . . . . .	9-12
§9.3.4. Strain-Displacement Relations . . . . .	9-12
§9.3.5. *Consistent Linearization . . . . .	9-13
§9.4. <b>Arbitrary Reference Configuration</b>	9-14
§9.4.1. Strain-Displacement Matrix . . . . .	9-14
§9.4.2. Constitutive Equations . . . . .	9-15
§9.4.3. Strain Energy . . . . .	9-16
§9.5. <b>The Internal Force</b>	9-16
§9.6. <b>The Stiffness Matrix</b>	9-17
§9.6.1. The Material Stiffness Matrix . . . . .	9-17
§9.6.2. Eliminating Shear Locking by RBF . . . . .	9-18
§9.6.3. The Geometric Stiffness Matrix . . . . .	9-19
§9.7. <b>A Commentary on the Element Performance</b>	9-21
§9.8. <b>Summary</b>	9-22
§9. <b>Exercises</b> . . . . .	9-23

## §9.1. Introduction

In the present Chapter the Standard Formulation of Total Lagrangian (TL) kinematics is used to derive the finite element equations of a two-node Timoshenko plane beam element. This derivation is more typical of the general case. It is still short, however, of the enormous complexity involved, for instance, in the FEM analysis of nonlinear three-dimensional beams or shells. In fact the latter are still doctoral thesis topics.

In the formulation of the bar element in Chapter 8, advantage was taken of the direct expression of the axial strain in terms of reference and current element lengths. That shortcut bypasses the use of displacement gradients and coordinate transformations. The simplification works equally well for bars in three-dimensional space.

A more systematic but lengthier procedure is unavoidable with more complicated elements. The procedure requires going through the displacement gradients to construct a strain measure. Sometimes this measure is too complex and must be simplified while retaining physical correctness. Then the stresses are introduced and paired with strains to form the strain energy function of the element. Repeated differentiations with respect to node displacements yield the expressions of the internal force vector and tangent stiffness matrix. Finally, a transformation to the global coordinate system may be required.

In addition to giving a better picture of the general procedure, the beam element offers an illustration of the treatment of rotational degrees of freedom.

## §9.2. Beam Models

### §9.2.1. Basic Concepts and Terminology

Beams represent the most common structural component found in civil and mechanical structures. Because of their ubiquity they are extensively studied, from an analytical viewpoint, in Mechanics of Materials courses. Such a basic knowledge is assumed here. The following material recapitulates definitions and concepts that are needed in the finite element formulation.

A *beam* is a rod-like structural member that can resist *transverse* loading applied between its supports. By “rod-like” it is meant that one of the dimensions is considerably larger than the other two. This dimension is called the *longitudinal dimension* and defines the *longitudinal direction* or *axial direction*. Directions normal to the longitudinal directions are called *transverse*. The intersection of planes normal to the longitudinal direction with the beam are called *cross sections*, just as for bar elements. The beam *longitudinal axis* is directed along the longitudinal direction and passes through the centroid of the cross sections.<sup>1</sup>

Beams may be used as isolated structures. But they can also be combined to form *framework* structures. This is actually the most common form of high-rise building construction. Individual beam components of a framework are called *members*, which are connected at *joints*. Frameworks

---

<sup>1</sup> If the beam is built of several materials, as in the case of reinforced concrete, the longitudinal axis passes through the centroid of a modified cross section. The modified-area technique is explained in elementary courses of Mechanics of Materials

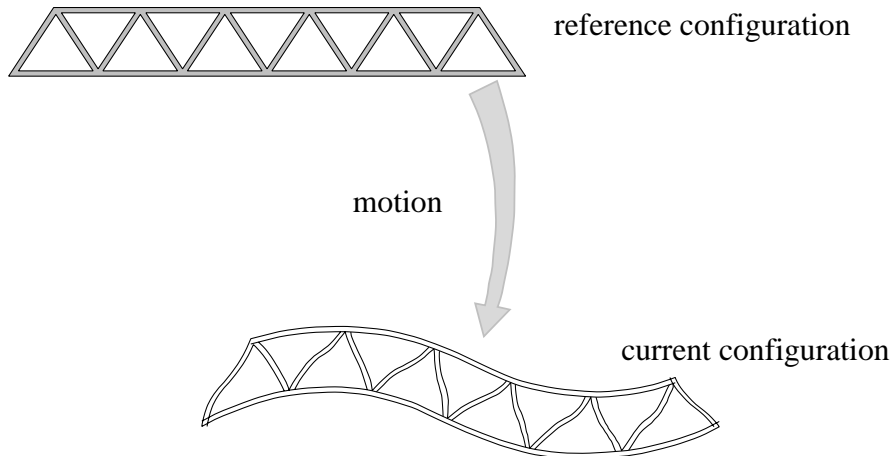


Figure 9.1. A geometrically nonlinear plane framework structure.

can be distinguished from trusses by the fact that their joints are sufficiently rigid to transmit bending moments between members.

In practical structures beam members can take up a great variety of loads, including biaxial bending, transverse shears, axial forces and even torsion. Such complicated actions are typical of *spatial beams*, which are used in three-dimensional frameworks and are subject to forces applied along arbitrary directions.

A *plane beam* resists primarily loading applied in one plane and has a cross section that is symmetric with respect to that plane. Plane frameworks, such as the one illustrated in Figure 9.1, are assemblies of plane beams that share that symmetry. Those structures can be analyzed with two-dimensional idealizations.

A beam is *straight* if the longitudinal direction is a straight line. A beam is *prismatic* if the cross section is uniform. Only straight, prismatic, plane beams will be considered in this Chapter.

### §9.2.2. Mathematical Models: Classical and Timoshenko

Beams are actually three-dimensional solids. One-dimensional mathematical models of plane beams are constructed on the basis of *beam theories*. All such theories involve some form of approximation that describes the behavior of the cross sections in terms of quantities *evaluated at the longitudinal axis*. More precisely, the element kinematics of a plane beam is completely defined if the following functions are given: the axial displacement  $u_X(X)$ , the transverse displacement  $u_Y(X)$  and the cross section rotation  $\theta_Z(X) \equiv \theta(X)$ , where  $X$  denotes the longitudinal coordinate in the reference configuration. See Figure 9.2.

Two beam models are in common use in structural mechanics:

*Euler-Bernoulli (EB) Model.* This is also called *classical beam theory* or the *engineering beam theory* and is the one covered in elementary treatments of Mechanics of Materials. This model accounts for bending moment effects on stresses and deformations. Transverse shear forces are recovered from equilibrium but their effect on beam deformations is neglected. Its fundamental assumption is that cross sections remain plane and *normal* to the deformed longitudinal axis. This

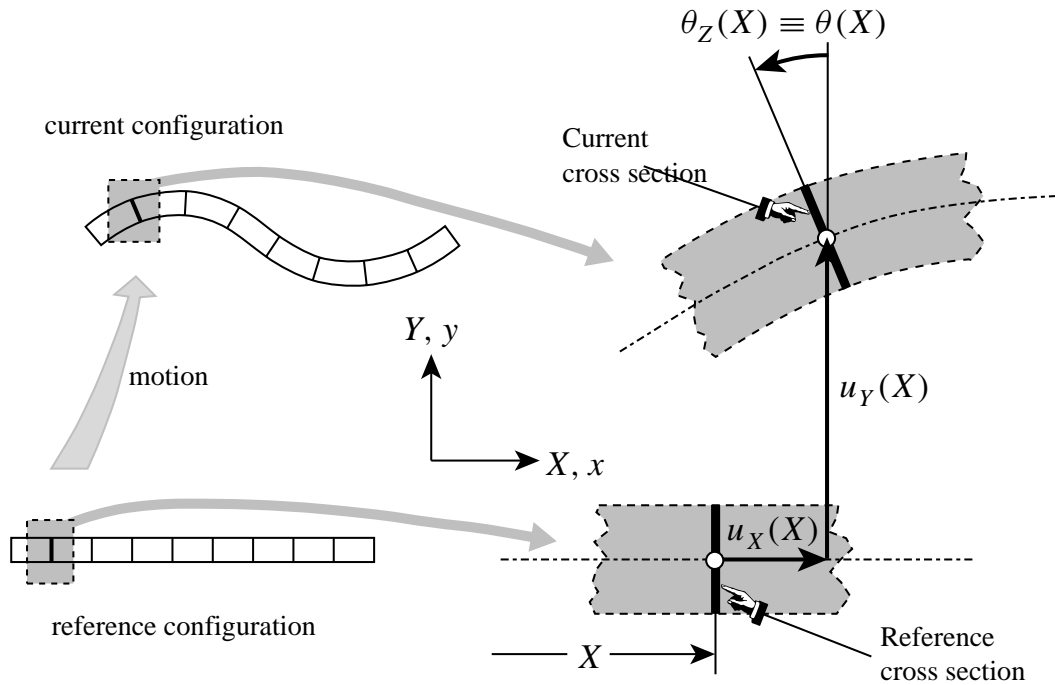


Figure 9.2. Definition of beam kinematics in terms of the three displacement functions  $u_X(X)$ ,  $u_Y(X)$  and  $\theta(X)$ . The figure actually depicts the EB model kinematics. In the Timoshenko model,  $\theta(X)$  is not constrained by normality (see next figure).

rotation occurs about a *neutral axis* that passes through the centroid of the cross section.

*Timoshenko Model.* This model corrects the classical beam theory with first-order shear deformation effects. In this theory cross sections remain plane and rotate about the same neutral axis as the EB model, but do not remain normal to the deformed longitudinal axis. The deviation from normality is produced by a transverse shear that is assumed to be constant over the cross section.

Both the EB and Timoshenko models rest on the assumptions of small deformations and linear-elastic isotropic material behavior. In addition both models neglect changes in dimensions of the cross sections as the beam deforms. Either theory can account for geometrically nonlinear behavior due to large displacements and rotations as long as the other assumptions hold.

### §9.2.3. Finite Element Models

To carry out the geometrically nonlinear finite element analysis of a framework structure, beam members are idealized as the assembly of one or more finite elements, as illustrated in Figure 9.3. The most common elements used in practice have two end nodes. The  $i^{th}$  node has three degrees of freedom: two node displacements  $u_{Xi}$  and  $u_{Yi}$ , and one nodal rotation  $\theta_i$ , positive counterclockwise in radians, about the Z axis. See Figure 9.4.

The cross section rotation from the reference to the current configuration is called  $\theta$  in both models. In the BE model this is the same as the rotation  $\psi$  of the longitudinal axis. In the Timoshenko

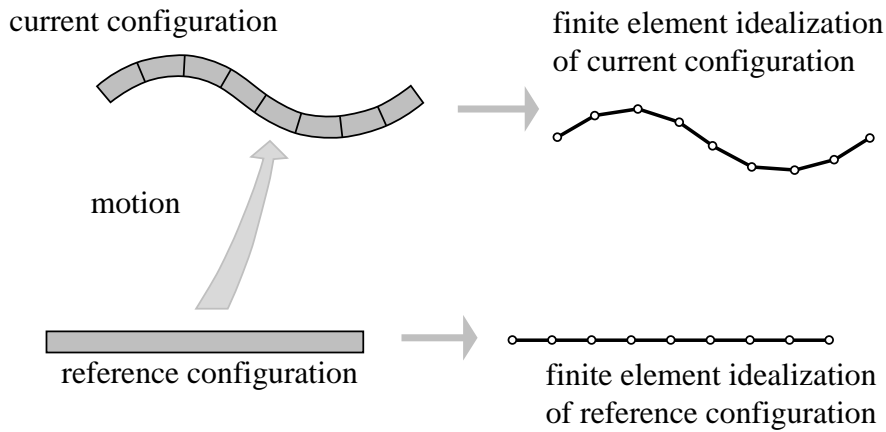


Figure 9.3. Idealization of a geometrically nonlinear beam member (as taken, for example, from a plane framework structure like the one in Figure 9.1) as an assembly of finite elements.

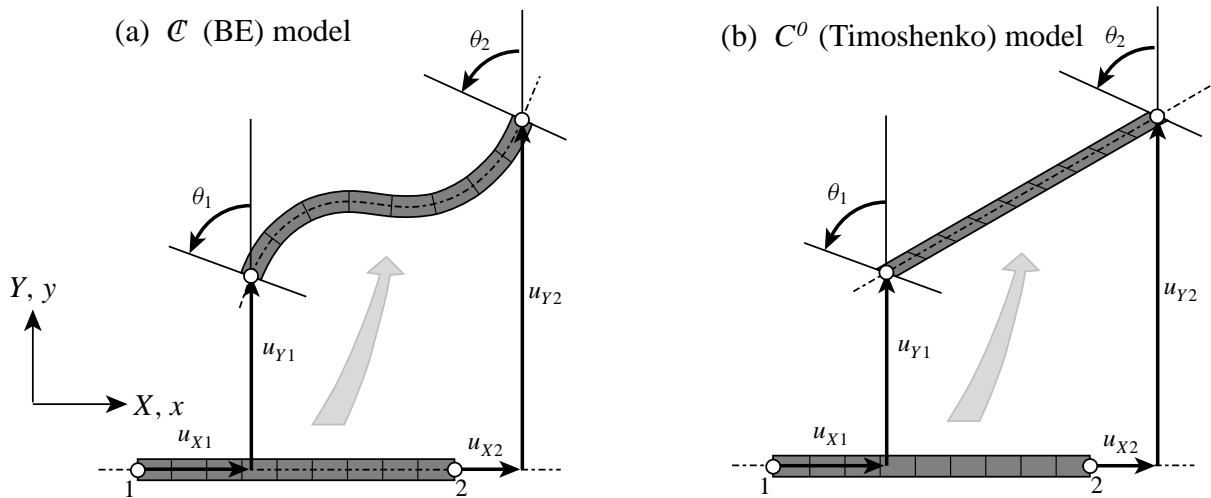
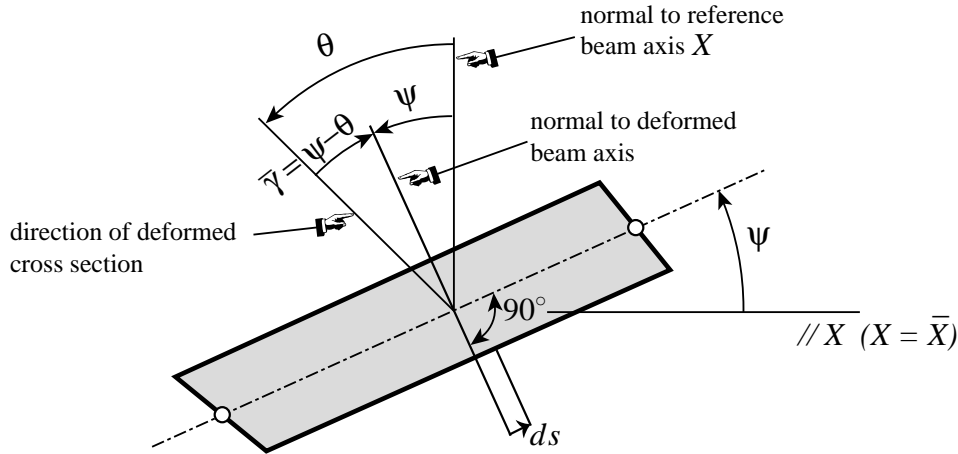


Figure 9.4. Two-node beam elements have six DOFs, regardless of the model used.

model, the difference  $\bar{\gamma} = \psi - \theta$  is used as measure of mean shear distortion.<sup>2</sup> These angles are illustrated in Figure 9.5.

Either the EB or the Timoshenko model may be used as the basis for the element formulation. Superficially it appears that one should select the latter only when shear effects are to be considered, as in “deep beams” whereas the EB model is used for ordinary beams. But here a “twist” appear because of finite element considerations. This twist is one that has caused significant confusion among FEM users over the past 25 years.

<sup>2</sup> It is  $\psi - \theta$  instead of  $\theta - \psi$  because of sign convention, to make  $e_{XY}$  positive.



Note: in practice  $\bar{\gamma} \ll \theta$ ; typically 0.1% or less. The magnitude of  $\bar{\gamma}$  is grossly exaggerated in the figure for visualization convenience.

Figure 9.5. Definition of total section rotation  $\theta$  and BE section rotation  $\psi$  in the Timoshenko beam model. The mean shear deformation is  $\bar{\gamma} = \theta - \psi$ , which is constant over the cross section. For small deformations of typical engineering materials  $\bar{\gamma} \ll 1$ ; for example, typical values for  $|\bar{\gamma}|$  are  $O(10^{-4})$  radians whereas rotations  $\psi$  and  $\theta$  may be of the order of several radians.

Although the Timoshenko beam model appears to be more complex because of the inclusion of shear deformation, finite elements based on this model are in fact simpler to construct! Here are the two main reasons:

- (i) Separate kinematic assumptions on the variation of cross-section rotations are possible, as made evident by Figure 9.5. Mathematically:  $\theta(X)$  may be assumed independently of  $u_X(X)$  and  $u_Y(X)$ . As a consequence, two-node Timoshenko elements may use *linear* variations in both displacement and rotations. On the other hand a two-node EB model requires a *cubic* polynomial for  $u_Y(X)$  because the rotation  $\theta(X)$  is not independent.
- (ii) The linear transverse displacement variation matches that commonly assumed for the axial deformation (bar-like behavior). The transverse and axial displacements are then said to be *consistent*.

The simplicity is even more important in geometrically nonlinear analysis, as strikingly illustrated in the two-node elements depicted in Figure 9.6. Although as shown in that figure both of these elements have six degrees of freedom, the internal kinematics of the Timoshenko model is far simpler.

#### §9.2.4. Bernoulli-Euler versus Timoshenko Beam Elements

In the FEM literature, a BE-based model such as the one shown in Figure 9.4(a) is called a  $C^1$  beam because this is the kind of mathematical continuity achieved in the longitudinal direction when a beam member is divided into several elements (cf. Figure 9.3). On the other hand the Timoshenko-based element shown in Figure 9.4(b) is called a  $C^0$  beam because both transverse displacements, as well as the rotation, preserve only  $C^0$  continuity.

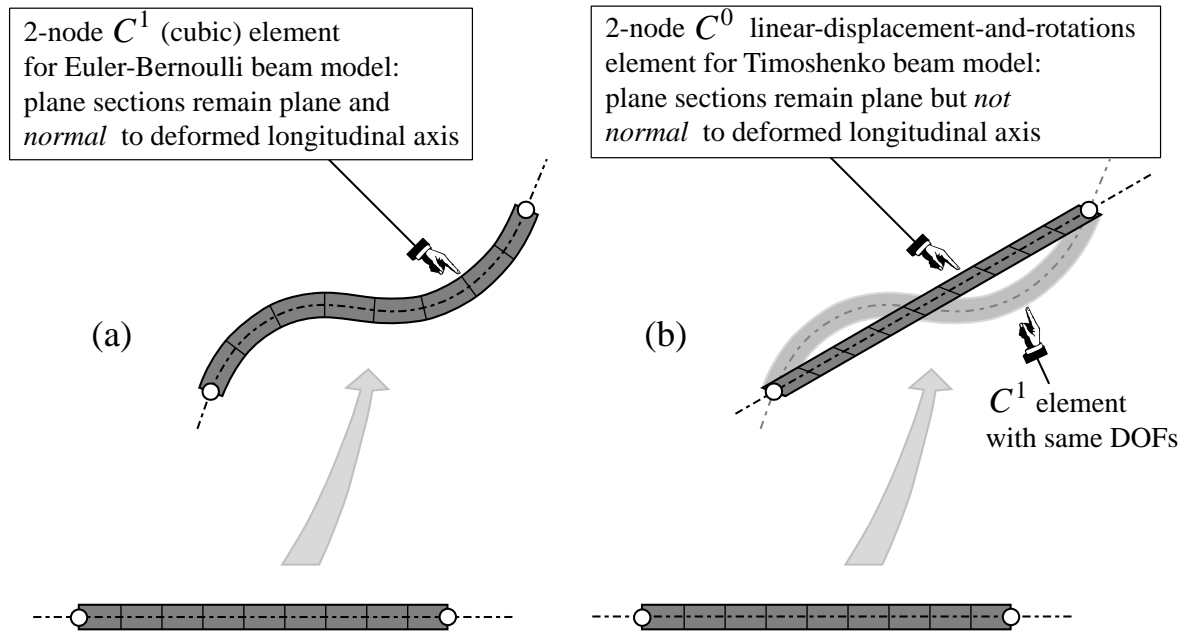


Figure 9.6. Sketch of the kinematics of two-node beam finite element models based on (a) Euler-Bernoulli beam theory, and (b) Timoshenko beam theory. These models are called  $C^1$  and  $C^0$  beams, respectively, in the FEM literature.

What would be the first reaction of an experienced but old-fashioned (i.e., “never heard about FEM”) structural engineer on looking at Figure 9.6? The engineer would pronounce the  $C^0$  element unsuitable for practical use. And indeed the kinematics looks strange. The shear distortion implied by the drawing appears to grossly violate the basic assumptions of beam behavior. Furthermore, a huge amount of shear energy would be required to keep the element straight as depicted.

The engineer would be both right and wrong. If the two-node element of Figure 9.6(b) were constructed with actual shear properties and exact integration, an overstiff model results. This phenomenon is well known in the FEM literature and receives the name of *shear locking*. To avoid locking while retaining the element simplicity it is necessary to use certain computational devices. The most common are:

1. Selective integration for the shear energy.
2. Residual energy balancing.

These devices will be used without explanation in some of the derivations of this Chapter. For detailed justification the curious reader may consult advanced FEM books such as Hughes'.<sup>3</sup>

In this Chapter the  $C^0$  model will be used to illustrate the TL formulation of a two-node, geometrically nonlinear beam element.

**Remark 9.1.** As a result of the application of the aforementioned devices the beam element behaves like a BE beam although the underlying model is Timoshenko's. This represents a curious paradox: shear deformation

<sup>3</sup> T. J. R. Hughes, *The Finite Element Method*, Prentice-Hall, 1987.

is used to simplify the kinematics, but then most of the shear is removed to restore the correct stiffness.<sup>4</sup> As a result, the name “ $C^0$  element” is more appropriate than “Timoshenko element” because capturing the actual shear deformation is not the main objective.

**Remark 9.2.** The two-node  $C^1$  beam element is used primarily in linear structural mechanics. (It is in fact the beam model used in the “Introduction to FEM” course.) This is because some of the easier-construction advantages cited for the  $C^0$  element are less noticeable, while no artificial devices to eliminate locking are needed. The  $C^1$  element is also called the *Hermitian beam element* because the shape functions are cubic polynomials specified by Hermite interpolation formulas.

### §9.3. X-Aligned Reference Configuration

#### §9.3.1. Element Description

We consider a two-node, straight, prismatic  $C^0$  plane beam element moving in the  $(X, Y)$  plane, as depicted in Figure 9.7(a). For simplicity in the following derivation the  $X$  axis system is initially aligned with the longitudinal direction in the reference configuration, with origin at node 1. This assumption is relaxed in the following section, once invariant strain measures are obtained.

The reference element length is  $L_0$ . The cross section area  $A_0$  and second moment of inertia  $I_0$  with respect to the neutral axis<sup>5</sup> are defined by the area integrals

$$A_0 = \int_{A_0} dA, \quad \int_{A_0} Y dA = 0, \quad I_0 = \int_{A_0} Y^2 dA, \quad (9.1)$$

In the current configuration those quantities become  $A$ ,  $I$  and  $L$ , respectively, but only  $L$  is frequently used in the TL formulation. The material remains linearly elastic with elastic modulus  $E$  relating the stress and strain measures defined below.

As in the previous Chapter the identification superscript ( $e$ ) will be omitted to reduce clutter until it is necessary to distinguish elements within structural assemblies.

The element has the six degrees of freedom depicted in Figure 9.4. These degrees of freedom and the associated node forces are collected in the node displacement and node force vectors

$$\mathbf{u} = \begin{bmatrix} u_{X1} \\ u_{Y1} \\ \theta_1 \\ u_{X2} \\ u_{Y2} \\ \theta_2 \end{bmatrix}, \quad \mathbf{f} = \begin{bmatrix} f_{X1} \\ f_{Y1} \\ f_{\theta1} \\ f_{X2} \\ f_{Y2} \\ f_{\theta2} \end{bmatrix}. \quad (9.2)$$

The loads acting on the nodes will be assumed to be conservative.

<sup>4</sup> The FEM analysis of plates and shells is also rife with such paradoxes.

<sup>5</sup> For a plane prismatic beam, the neutral axis at a particular section is the intersection of the cross section plane  $X = \text{constant}$  with the plane  $Y = 0$ .

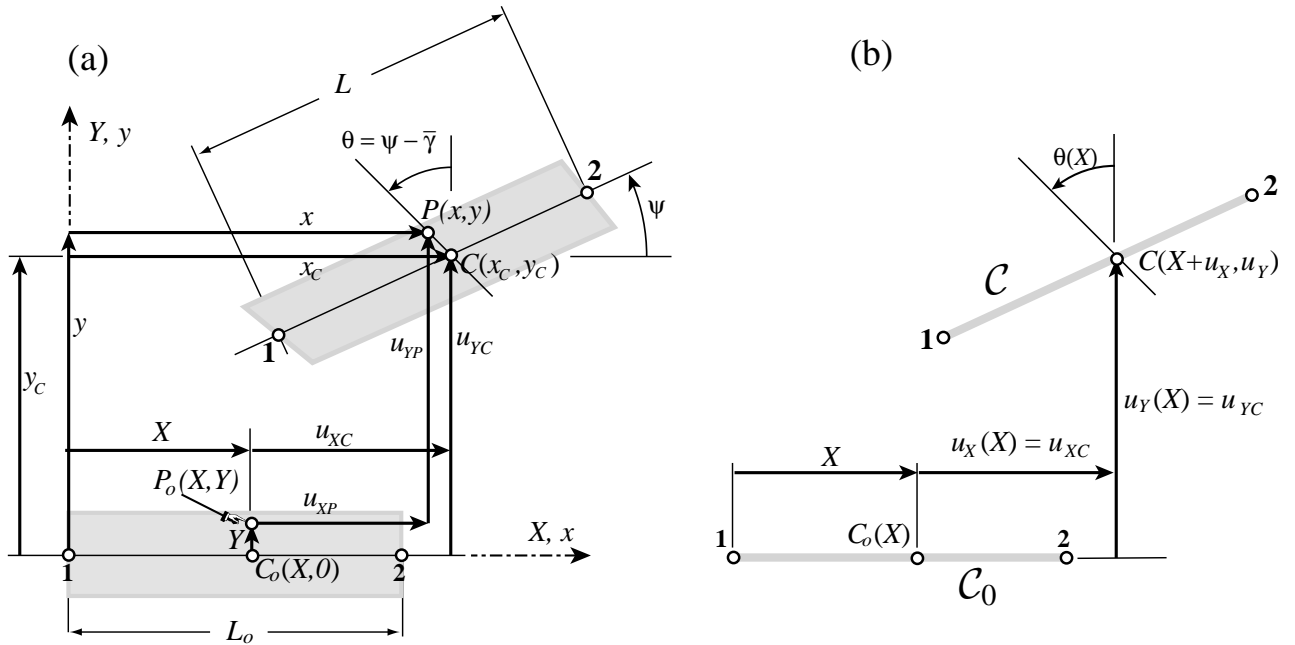


Figure 9.7. Lagrangian kinematics of the  $C^0$  beam element with  $X$ -aligned reference configuration: (a) plane beam moving as a two-dimensional body; (b) reduction of motion description to one dimension measured by coordinate  $X$ .

§9.3.2. Motion

The kinematic assumptions of the Timoshenko model element have been outlined in §9.2.2. Basically they state that cross sections remain plane upon deformation but not necessarily normal to the deformed longitudinal axis. In addition, changes in cross section geometry are neglected.

To analyze the Lagrangian kinematics of the element shown in Figure 9.6(a), we study the motion of a particle originally located at  $P_0(X, Y)$ . The particle moves to  $P(x, y)$  in the current configuration. The projections of  $P_0$  and  $P$  along the cross sections at  $C_0$  and  $C$  upon the neutral axis are called  $C_0(X, 0)$  and  $C(x_C, y_C)$ , respectively. We shall assume that the beam cross section dimensions do not change, and that the shear distortion  $\gamma \ll 1$  so that  $\cos \gamma$  can be replaced by 1. Then

$$\begin{aligned} x &= x_C - Y(\sin \psi + \sin \gamma \cos \psi) = x_C - Y[\sin(\psi + \gamma) + (1 - \cos \gamma) \sin \psi] \doteq x_C - Y \sin \theta, \\ y &= y_C + Y(\cos \psi - \sin \gamma \sin \psi) = y_C + Y[\cos(\psi + \gamma) + (1 - \cos \gamma) \cos \psi] \doteq y_C + Y \cos \theta. \end{aligned} \tag{9.3}$$

But  $x_C = X + u_{XC}$  and  $y_C = u_{YC}$ . Consequently  $x = X + u_{XC} - Y \sin \theta$  and  $y = u_{YC} + Y \cos \theta$ . From now we shall call  $u_{XC}$  and  $u_{YC}$  simply  $u_X$  and  $u_Y$ , respectively, so that the Lagrangian representation of the motion is

$$\boxed{\begin{bmatrix} x \\ y \end{bmatrix} = \begin{bmatrix} X + u_X - Y \sin \theta \\ u_Y + Y \cos \theta \end{bmatrix}} \tag{9.4}$$

in which  $u_X$ ,  $u_Y$  and  $\theta$  are functions of  $X$  only. This concludes the reduction to a one-dimensional model, as sketched in Figure 9.7(b).

For future use below it is convenient to define an “extended” internal displacement vector  $\mathbf{w}$ , and its gradient or  $X$  derivative:

$$\mathbf{w} = \begin{bmatrix} u_X(X) \\ u_Y(X) \\ \theta(X) \end{bmatrix}, \quad \mathbf{w}' = \frac{d\mathbf{w}}{dX} = \begin{bmatrix} du_X/dX \\ du_Y/dX \\ d\theta/dX \end{bmatrix} = \begin{bmatrix} u'_X \\ u'_Y \\ \theta' \end{bmatrix}, \quad (9.5)$$

in which primes denote derivatives with respect to  $X$ . The derivative  $\theta'$  is also as  $\kappa$ , which has the meaning of beam curvature in the current configuration. Also useful are the following differential relations

$$1 + u'_X = s' \cos \psi, \quad u'_Y = s' \sin \psi, \quad s' = \frac{ds}{dX} = \sqrt{(1 + u'_X)^2 + (u'_Y)^2}, \quad (9.6)$$

in which  $ds$  is the differential arclength in the current configuration; see Figure 9.5. If  $u'_X$  and  $u'_Y$  are constant over the element,

$$s' = L/L_0, \quad 1 + u'_X = L \cos \psi/L_0, \quad u'_Y = L \sin \psi/L_0. \quad (9.7)$$

**Remark 9.3.** The replacement of  $1 - \cos \gamma$  by zero in (9.3) is equivalent to saying that  $Y(1 - \cos \gamma)$  can be neglected in comparison to other cross section dimensions. This is consistent with the uncertainty in the cross section changes, which would depend on the normal stress and Poisson’s ratio effects. The motion expression (9.4) has the virtue of being purely kinematic and of leading to (exactly)  $e_{\gamma Y} = 0$ .

### §9.3.3. Displacement Interpolation

For a 2-node  $C^0$  element it is natural to express the displacements and rotation functions as linear in the node displacements:

$$\mathbf{w} = \begin{bmatrix} u_X(X) \\ u_Y(X) \\ \theta(X) \end{bmatrix} = \frac{1}{2} \begin{bmatrix} 1 - \xi & 0 & 0 & 1 + \xi & 0 & 0 \\ 0 & 1 - \xi & 0 & 0 & 1 + \xi & 0 \\ 0 & 0 & 1 - \xi & 0 & 0 & 1 + \xi \end{bmatrix} \begin{bmatrix} u_{X1} \\ u_{Y1} \\ \theta_1 \\ u_{X2} \\ u_{Y2} \\ \theta_2 \end{bmatrix} = \mathbf{N} \mathbf{u}, \quad (9.8)$$

in which  $\xi = (2X/L_0) - 1$  is the isoparametric coordinate that varies from  $\xi = -1$  at node 1 to  $\xi = 1$  at node 2. Differentiating this expression with respect to  $X$  yields the gradient interpolation:

$$\mathbf{w}' = \begin{bmatrix} u'_X \\ u'_Y \\ \theta' \end{bmatrix} = \frac{1}{L_0} \begin{bmatrix} -1 & 0 & 0 & 1 & 0 & 0 \\ 0 & -1 & 0 & 0 & 1 & 0 \\ 0 & 0 & -1 & 0 & 0 & 1 \end{bmatrix} \begin{bmatrix} u_{X1} \\ u_{Y1} \\ \theta_1 \\ u_{X2} \\ u_{Y2} \\ \theta_2 \end{bmatrix} = \mathbf{G} \mathbf{u}. \quad (9.9)$$

### §9.3.4. Strain-Displacement Relations

The deformation matrix of the motion (9.4) is

$$\mathbf{F} = \begin{bmatrix} \frac{\partial x}{\partial X} & \frac{\partial x}{\partial Y} \\ \frac{\partial y}{\partial X} & \frac{\partial y}{\partial Y} \end{bmatrix} = \begin{bmatrix} 1 + u'_X - Y\kappa \cos \theta & -\sin \theta \\ u'_Y - Y\kappa \sin \theta & \cos \theta \end{bmatrix} \quad (9.10)$$

where primes denote derivatives with respect to  $X$ , and  $\kappa = \theta'$ . The displacement gradient matrix is<sup>6</sup>

$$\mathbf{G}_F = \mathbf{F} - \mathbf{I} = \begin{bmatrix} u'_X - Y\kappa \cos \theta & -\sin \theta \\ u'_Y - Y\kappa \sin \theta & \cos \theta - 1 \end{bmatrix}, \quad (9.11)$$

from which the Green-Lagrange (GL) strain tensor follows:

$$\begin{aligned} \underline{\mathbf{e}} &= \begin{bmatrix} e_{XX} & e_{XY} \\ e_{YX} & e_{YY} \end{bmatrix} = \frac{1}{2}(\mathbf{F}^T \mathbf{F} - \mathbf{I}) = \frac{1}{2}(\mathbf{G}_F + \mathbf{G}_F^T) + \frac{1}{2}\mathbf{G}_F^T \mathbf{G}_F \\ &= \frac{1}{2} \begin{bmatrix} 2(u'_X - Y\kappa \cos \theta) + (u'_X - Y\kappa \cos \theta)^2 + (u'_Y - Y\kappa \sin \theta)^2 & -(1 + u'_X) \sin \theta + u'_Y \cos \theta \\ -(1 + u'_X) \sin \theta + u'_Y \cos \theta & 0 \end{bmatrix} \end{aligned} \quad (9.12)$$

It is seen that the only nonzero strains are the axial strain  $e_{XX}$  and the shear strain  $e_{XY} + e_{YX} = 2e_{XY}$ , whereas  $e_{YY}$  vanishes. Through the consistent-linearization techniques described in the subsection

<sup>6</sup> This is denoted by  $\mathbf{G}_F$  to avoid clash with the shape function gradient matrix  $\mathbf{G} = \mathbf{N}'$  introduced in (9.9).

below, it can be shown that under the small-strain assumptions made precise therein, the axial strain  $e_{XX}$  can be replaced by the simpler form

$$e_{XX} = (1 + u'_X) \cos \theta + u'_Y \sin \theta - Y\kappa - 1, \quad (9.13)$$

in which all quantities appear linearly except  $\theta$ . The nonzero axial and shear strains will be arranged in the strain vector

$$\mathbf{e} = \begin{bmatrix} e_1 \\ e_2 \end{bmatrix} = \begin{bmatrix} e_{XX} \\ 2e_{XY} \end{bmatrix} = \begin{bmatrix} (1 + u'_X) \cos \theta + u'_Y \sin \theta - Y\theta' - 1 \\ -(1 + u'_X) \sin \theta + u'_Y \cos \theta \end{bmatrix} = \begin{bmatrix} e - Y\kappa \\ \gamma \end{bmatrix}. \quad (9.14)$$

The three strain quantities introduced in (9.14):

$$e = (1 + u'_X) \cos \theta + u'_Y \sin \theta - 1, \quad \gamma = -(1 + u'_X) \sin \theta + u'_Y \cos \theta, \quad \kappa = \theta', \quad (9.15)$$

characterize axial strains, shear strains and curvatures, respectively. These are collected in the following generalized strain vector:

$$\mathbf{h}^T = [e \quad \gamma \quad \kappa] \quad (9.16)$$

Because of the assumed linear variation in  $X$  of  $u_X(X)$ ,  $u_Y(X)$  and  $\theta(X)$ ,  $e$  and  $\gamma$  only depend on  $\theta$  whereas  $\kappa$  is constant over the element. Making use of the relations (9.7) one can express  $e$  and  $\gamma$  in the geometrically invariant form

$$1 + e = s' \cos(\theta - \psi) = \frac{L \cos \bar{\gamma}}{L_0}, \quad \gamma = -s' \sin(\theta - \psi) = \frac{L \sin \bar{\gamma}}{L_0} \quad (9.17)$$

In theory one could further reduce  $e$  to  $L/L_0$  and  $\gamma$  to  $L\bar{\gamma}/L_0$ , but these “simplifications” actually complicate the strain variations taken in the following Section.

### §9.3.5. \*Consistent Linearization

The derivation of the consistent linearization (9.14) is based on the following study, known in continuum mechanics as a *polar decomposition* analysis of the deformation gradient. Introduce the matrix

$$\mathbf{\Omega}(\alpha) = \begin{bmatrix} \cos \alpha & -\sin \alpha \\ \sin \alpha & \cos \alpha \end{bmatrix} \quad (9.18)$$

which represents a two-dimensional rotation (about  $Z$ ) through an angle  $\alpha$ . Since  $\mathbf{\Omega}$  is an orthogonal matrix,  $\mathbf{\Omega}^T = \mathbf{\Omega}^{-1}$ . The deformation gradient (9.9) can be written

$$\mathbf{F} = \mathbf{\Omega}(\psi) \begin{bmatrix} s' & 0 \\ 0 & 0 \end{bmatrix} + \mathbf{\Omega}(\theta) \begin{bmatrix} -Y\theta' & 0 \\ 0 & 1 \end{bmatrix}. \quad (9.19)$$

where  $s'$  is defined in (9.6). Premultiplying both sides of (9.19) by  $\mathbf{\Omega}(-\theta)$  gives the modified deformation gradient

$$\bar{\mathbf{F}} = \mathbf{\Omega}(-\theta)\mathbf{F} = \begin{bmatrix} s' \cos(\theta - \psi) - Y\theta' & 0 \\ -s' \sin(\theta - \psi) & 1 \end{bmatrix} \quad (9.20)$$

Now the GL strain tensor  $2\mathbf{e} = \mathbf{F}^T \mathbf{F} - \mathbf{I}$  does not change if  $\mathbf{F}$  is premultiplied by an orthogonal matrix  $\mathbf{\Omega}$  because  $\mathbf{F}^T \mathbf{\Omega}^T \mathbf{\Omega} \mathbf{F} = \mathbf{F}^T \mathbf{F}$ . Consequently  $2\mathbf{e} = \bar{\mathbf{F}}^T \bar{\mathbf{F}} - \mathbf{I}$ . But if the strains remain small, as it is assumed in the Timoshenko model, the following are small quantities:

- (i)  $s' - 1 = (L/L_0) - 1$  because the axial strains are small;
- (ii)  $Y\theta' = Y\kappa$  because the curvature  $\kappa$  is of order  $1/R$ ,  $R$  being the radius of curvature, and  $|R| \gg |Y|$  according to beam theory because  $Y$  can vary only up to the cross section in-plane dimension;
- (iii)  $\bar{\gamma} = \psi - \theta$ , which is the mean angular shear deformation.

Then  $\bar{\mathbf{F}} = \mathbf{I} + \mathbf{L}$  + higher order terms, where  $\mathbf{L}$  is a first-order linearization in the small quantities  $s' - 1$ ,  $Y\theta'$  and  $\bar{\gamma} = \psi - \theta$ . It follows that

$$\mathbf{e} = \frac{1}{2}(\mathbf{L} + \mathbf{L}^T) + \text{higher order terms} \quad (9.21)$$

Carrying out this linearization one finds that  $e_{XY}$  and  $e_{YY}$  do not change, but that  $e_{XX}$  simplifies to (9.13). It can also be shown that  $2e_{XY} = \gamma \doteq \bar{\gamma}$  within the order of approximation of (9.21).

### §9.4. Arbitrary Reference Configuration

In the general case the reference configuration  $\mathcal{C}_0$  of the element is not aligned with  $X$ . The longitudinal axis  $\bar{X}$  forms an angle  $\varphi$  with  $X$ , as illustrated in Figure 9.8. The six degrees of freedom of the element are indicated in that Figure. Note that the section rotation angle  $\theta$  is measured from the direction  $\bar{Y}$ , normal to  $\bar{X}$ , and no longer from  $Y$  as in Figure 9.6.

Given the node coordinates  $(X_1, Y_1)$  and  $(X_2, Y_2)$ , the reference angle  $\varphi$  is determined by

$$\cos \varphi = X_{21}/L_0, \quad \sin \varphi = Y_{21}/L_0, \quad X_{21} = X_2 - X_1, \quad Y_{21} = Y_2 - Y_1, \quad L_0^2 = X_{21}^2 + Y_{21}^2. \quad (9.22)$$

The angle  $\phi = \psi + \varphi$  formed by the current longitudinal axis with  $X$  (see Figure 9.12) is determined by

$$\begin{aligned} \cos \phi &= \cos(\psi + \varphi) = x_{21}/L, \quad \sin \phi = \sin(\psi + \varphi) = y_{21}/L, \quad \text{with} \\ x_{21} &= x_2 - x_1 = X_{21} + u_{X2} - u_{X1}, \quad y_{21} = y_2 - y_1 = Y_{21} + u_{Y2} - u_{Y1}, \quad L^2 = x_{21}^2 + y_{21}^2. \end{aligned} \quad (9.23)$$

Solving the trigonometric relations (9.22)-(9.23) for  $\psi$  gives

$$\begin{aligned} \cos \psi &= \frac{X_{21}x_{21} + Y_{21}y_{21}}{LL_0} = \frac{X_{21}(X_{21} + u_{X2} - u_{X1}) + Y_{21}(Y_{21} + u_{Y2} - u_{Y1})}{LL_0}, \\ \sin \psi &= \frac{X_{21}y_{21} - Y_{21}x_{21}}{LL_0} = \frac{X_{21}(Y_{21} + u_{Y2} - u_{Y1}) - Y_{21}(X_{21} + u_{X2} - u_{X1})}{LL_0}. \end{aligned} \quad (9.24)$$

It follows that  $L \sin \psi$  and  $L \cos \psi$  are exactly *linear* in the translational node displacements. This property simplifies considerably the calculations that follow.

#### §9.4.1. Strain-Displacement Matrix

For the generalized strains it is convenient to use the invariant form (9.17), which does not depend on  $\varphi$ . The variations  $\delta e$ ,  $\delta \gamma$  and  $\delta \kappa$  with respect to nodal displacement variations are required in the formation of the strain displacement relation  $\delta \mathbf{h} = \mathbf{B} \delta \mathbf{u}$ . To form  $\mathbf{B}$  we take partial derivatives of  $e$ ,  $\gamma$  and  $\kappa$  with respect to node displacements. Here is a sample of the kind of calculations involved:

$$\begin{aligned} \frac{\partial e}{\partial u_{X1}} &= \frac{\partial [L \cos(\theta - \psi)/L_0 - 1]}{\partial u_{X1}} = \frac{\partial [L(\cos \theta \cos \psi + \sin \theta \sin \psi)/L_0 - 1]}{\partial u_{X1}} \\ &= \frac{-X_{21} \cos \theta + Y_{21} \sin \theta}{L_0^2} = \frac{-\cos \varphi \cos \theta + \sin \varphi \sin \theta}{L_0} = -\frac{\cos \omega}{L_0} \end{aligned} \quad (9.25)$$

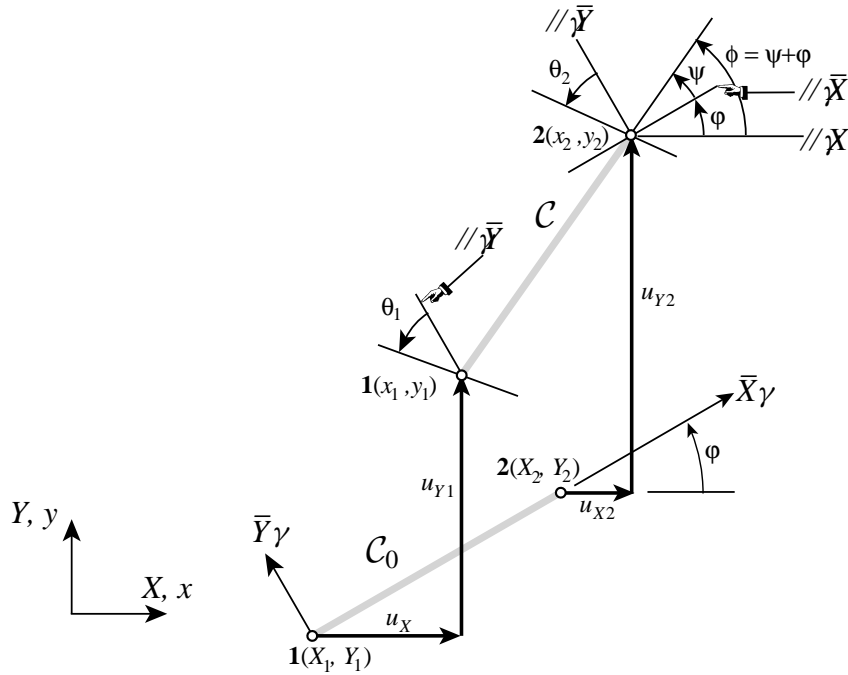


Figure 9.8. Plane beam element with arbitrarily oriented reference configuration.

in which  $\omega = \theta + \varphi$ , and where use is made of (9.24) in a key step. These derivatives were checked with *Mathematica*. Collecting all of them into matrix  $\mathbf{B}$ :

$$\mathbf{B} = \frac{1}{L_0} \begin{bmatrix} -\cos \omega & -\sin \omega & L_0 \mathcal{N}_1 \gamma & \cos \omega & \sin \omega & L_0 \mathcal{N}_2 \gamma \\ \sin \omega & -\cos \omega & -L_0 \mathcal{N}_1 (1 + e) & -\sin \omega & \cos \omega & -L_0 \mathcal{N}_2 (1 + e) \\ 0 & 0 & -1 & 0 & 0 & 1 \end{bmatrix}. \quad (9.26)$$

Here  $\mathcal{N}_1 = (1 - \xi)/2$  and  $\mathcal{N}_2 = (1 + \xi)/2$  are abbreviations for the element shape functions (caligraphic symbols are used to lessen the chance of clash against axial force symbols).

### §9.4.2. Constitutive Equations

Because the beam material is assumed to be homogeneous and isotropic, the only nonzero PK2 stresses are the axial stress  $s_{XX}$  and the shear stress  $s_{XY}$ . These are collected in a stress vector  $\mathbf{s}$  related to the GL strains by the linear elastic relations

$$\mathbf{s} = \begin{bmatrix} s_{XX} \\ s_{XY} \end{bmatrix} = \begin{bmatrix} s_1 \\ s_2 \end{bmatrix} = \begin{bmatrix} s_1^0 + E e_1 \\ s_2^0 + G e_2 \end{bmatrix} = \begin{bmatrix} s_1^0 \\ s_2^0 \end{bmatrix} + \begin{bmatrix} E & 0 \\ 0 & G \end{bmatrix} \begin{bmatrix} e_1 \\ e_2 \end{bmatrix} = \mathbf{s}^0 + \mathbf{E} \mathbf{e}, \quad (9.27)$$

where  $E$  is the modulus of elasticity and  $G$  is the shear modulus. We introduce the prestress resultants

$$N^0 = \int_{A_0} s_1^0 dA, \quad V^0 = \int_{A_0} s_2^0 dA, \quad M^0 = \int_{A_0} -Y s_1^0 dA, \quad (9.28)$$

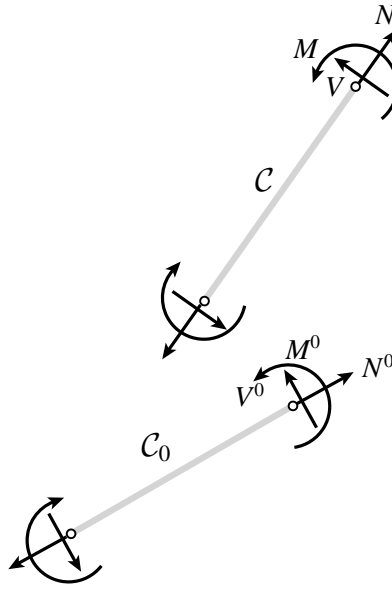


Figure 9.9. Beam stress resultants (internal forces) in the reference and current configurations.

which define the axial forces, transverse shear forces and bending moments, respectively, in the reference configuration. We also define the stress resultants

$$\boxed{N = N^0 + EA_0 e, \quad V = V^0 + GA_0 \gamma, \quad M = M^0 + EI_0 \kappa.} \quad (9.29)$$

These represent axial forces, transverse shear forces and bending moments in the current configuration, respectively, defined in terms of PK2 stresses. See Figure 9.9 for signs. These are collected in the stress-resultant vector

$$\mathbf{z}^T = [N \quad V \quad M]. \quad (9.30)$$

### §9.4.3. Strain Energy

As in the case of the bar element, the total potential energy  $\Pi = U - P$  is separable because  $P = \lambda \mathbf{q}^T \mathbf{u}$ . The strain (internal) energy is given by

$$U = \int_{V_0} [(\mathbf{s}^0)^T \mathbf{e} + \frac{1}{2} \mathbf{e}^T \mathbf{E} \mathbf{e}] dV = \int_{A_0} \int_{L_0} [(s_1^0 e_1 + s_2^0 e_2) + \frac{1}{2} (E e_1^2 + G e_2^2)] dA d\bar{X}. \quad (9.31)$$

Carrying out the area integrals while making use of (9.27) through (9.30),  $U$  can be written as the sum of three length integrals:

$$\boxed{U = \int_{L_0} (N^0 e + \frac{1}{2} EA_0 e^2) d\bar{X} + \int_{L_0} (V^0 \gamma + \frac{1}{2} GA_0 \gamma^2) d\bar{X} + \int_{L_0} (M^0 \kappa + \frac{1}{2} EI_0 \kappa^2) d\bar{X},} \quad (9.32)$$

The three terms in (9.32) define the energy stored through bar-like axial deformations, shear distortion and pure bending, respectively.

### §9.5. The Internal Force

The internal force vector can be obtained by taking the first variation of the internal energy with respect to the node displacements. This can be compactly expressed as

$$\delta U = \int_{L_0} (N \delta e + V \delta \gamma + M \delta \kappa) d\bar{X} = \int_{L_0} \mathbf{z}^T \delta \mathbf{h} d\bar{X} = \int_{L_0} \mathbf{z}^T \mathbf{B} d\bar{X} \delta \mathbf{u}. \quad (9.33)$$

Here  $\mathbf{h}$  and  $\mathbf{B}$  are defined in equations (9.16) and (9.26) whereas  $\mathbf{z}$  collects the stress resultants in  $\mathcal{C}$  as defined in (9.28) through (9.30). Because  $\delta U = \mathbf{p}^T \delta \mathbf{u}$ , we get

$$\mathbf{p} = \int_{L_0} \mathbf{B}^T \mathbf{z} d\bar{X}. \quad (9.34)$$

This expression may be evaluated by a one point Gauss integration rule with the sample point at  $\xi = 0$  (beam midpoint). Let  $\theta_m = (\theta_1 + \theta_2)/2$ ,  $\omega_m = \theta_m + \varphi$ ,  $c_m = \cos \omega_m$ ,  $s_m = \sin \omega_m$ ,  $e_m = L \cos(\theta_m - \psi)/L_0 - 1$ ,  $\gamma_m = L \sin(\psi - \theta_m)/L_0$ , and

$$\mathbf{B}_m = \mathbf{B}|_{\xi=0} = \frac{1}{L_0} \begin{bmatrix} -c_m & -s_m & -\frac{1}{2}L_0\gamma_m & c_m & s_m & -\frac{1}{2}L_0\gamma_m \\ s_m & -c_m & \frac{1}{2}L_0(1+e_m) & s_m & -c_m & \frac{1}{2}L_0(1+e_m) \\ 0 & 0 & -1 & 0 & 0 & 1 \end{bmatrix} \quad (9.35)$$

where subscript  $m$  stands for “beam midpoint.” Then

$$\mathbf{p} = L_0 \mathbf{B}_m^T \mathbf{z} = \begin{bmatrix} -c_m & -s_m & \frac{1}{2}L_0\gamma_m & c_m & s_m & -\frac{1}{2}L_0\gamma_m \\ s_m & -c_m & -\frac{1}{2}L_0(1+e_m) & -s_m & c_m & \frac{1}{2}L_0(1+e_m) \\ 0 & 0 & -1 & 0 & 0 & 1 \end{bmatrix}^T \begin{bmatrix} N \\ V \\ M \end{bmatrix} \quad (9.36)$$

### §9.6. The Stiffness Matrix

The first variation of the internal force vector (9.34) defines the tangent stiffness matrix

$$\delta \mathbf{p} = \int_{L_0} (\mathbf{B}^T \delta \mathbf{z} + \delta \mathbf{B}^T \mathbf{z}) d\bar{X} = (\mathbf{K}_M + \mathbf{K}_G) \delta \mathbf{u} = \mathbf{K} \delta \mathbf{u}. \quad (9.37)$$

This is again the sum of the material stiffness  $\mathbf{K}_M$  and the geometric stiffness  $\mathbf{K}_G$ .

#### §9.6.1. The Material Stiffness Matrix

The material stiffness comes from the variation  $\delta \mathbf{z}$  of the stress resultants while keeping  $\mathbf{B}$  fixed. This is easily obtained by noting that

$$\delta \mathbf{z} = \begin{bmatrix} \delta N \\ \delta V \\ \delta M \end{bmatrix} = \begin{bmatrix} EA_0 & 0 & 0 \\ 0 & GA_0 & 0 \\ 0 & 0 & EI_0 \end{bmatrix} \begin{bmatrix} \delta e \\ \delta \gamma \\ \delta \kappa \end{bmatrix} = \mathbf{S} \delta \mathbf{h}, \quad (9.38)$$

where  $\mathbf{S}$  is the diagonal constitutive matrix with entries  $EA_0$ ,  $GA_0$  and  $EI_0$ . Because  $\delta \mathbf{h} = \mathbf{B} \delta \mathbf{u}$ , the term  $\mathbf{B}^T \delta \mathbf{z}$  becomes  $\mathbf{B}^T \mathbf{S} \mathbf{B} \delta \mathbf{u} = \mathbf{K}_M \delta \mathbf{u}$  whence the material matrix is

$$\mathbf{K}_M = \int_{L_0} \mathbf{B}^T \mathbf{S} \mathbf{B} d\bar{X}. \quad (9.39)$$

This integral is evaluated by the one-point Gauss rule at  $\xi = 0$ . Denoting again by  $\mathbf{B}_m$  the matrix (9.35), we find

$$\mathbf{K}_M = \int_{L_0} \mathbf{B}_m^T \mathbf{S} \mathbf{B}_m d\bar{X} = \mathbf{K}_M^a + \mathbf{K}_M^b + \mathbf{K}_M^s \quad (9.40)$$

where  $\mathbf{K}_M^a$ ,  $\mathbf{K}_M^b$  and  $\mathbf{K}_M^s$  are due to axial (bar), bending, and shear stiffness, respectively:

$$\mathbf{K}_M^a = \frac{EA_0}{L_0} \begin{bmatrix} c_m^2 & c_m s_m & -c_m \gamma_m L_0/2 & -c_m^2 & -c_m s_m & -c_m \gamma_m L_0/2 \\ c_m s_m & s_m^2 & -\gamma_m L_0 s_m/2 & -c_m s_m & -s_m^2 & -\gamma_m L_0 s_m/2 \\ -c_m \gamma_m L_0/2 & -\gamma_m L_0 s_m/2 & \gamma_m^2 L_0^2/4 & c_m \gamma_m L_0/2 & \gamma_m L_0 s_m/2 & \gamma_m^2 L_0^2/4 \\ -c_m^2 & -c_m s_m & c_m \gamma_m L_0/2 & c_m^2 & c_m s_m & c_m \gamma_m L_0/2 \\ -c_m s_m & -s_m^2 & \gamma_m L_0 s_m/2 & c_m s_m & s_m^2 & \gamma_m L_0 s_m/2 \\ -c_m \gamma_m L_0/2 & -\gamma_m L_0 s_m/2 & \gamma_m^2 L_0^2/4 & c_m \gamma_m L_0/2 & \gamma_m L_0 s_m/2 & \gamma_m^2 L_0^2/4 \end{bmatrix} \quad (9.41)$$

$$\mathbf{K}_M^b = \frac{EI_0}{L_0} \begin{bmatrix} 0 & 0 & 0 & 0 & 0 & 0 \\ 0 & 0 & 0 & 0 & 0 & 0 \\ 0 & 0 & 1 & 0 & 0 & -1 \\ 0 & 0 & 0 & 0 & 0 & 0 \\ 0 & 0 & 0 & 0 & 0 & 0 \\ 0 & 0 & -1 & 0 & 0 & 1 \end{bmatrix} \quad (9.42)$$

$$\mathbf{K}_M^s = \frac{GA_0}{L_0} \begin{bmatrix} s_m^2 & -c_m s_m & -a_1 L_0 s_m/2 & -s_m^2 & c_m s_m & -a_1 L_0 s_m/2 \\ -c_m s_m & c_m^2 & c_m a_1 L_0/2 & c_m s_m & -c_m^2 & c_m a_1 L_0/2 \\ -a_1 L_0 s_m/2 & c_m a_1 L_0/2 & a_1^2 L_0^2/4 & a_1 L_0 s_m/2 & -c_m a_1 L_0/2 & a_1^2 L_0^2/4 \\ -s_m^2 & c_m s_m & a_1 L_0 s_m/2 & s_m^2 & -c_m s_m & a_1 L_0 s_m/2 \\ c_m s_m & -c_m^2 & -c_m a_1 L_0/2 & -c_m s_m & c_m^2 & -c_m a_1 L_0/2 \\ -a_1 L_0 s_m/2 & c_m a_1 L_0/2 & a_1^2 L_0^2/4 & a_1 L_0 s_m/2 & -c_m a_1 L_0/2 & a_1^2 L_0^2/4 \end{bmatrix} \quad (9.43)$$

in which  $a_1 = 1 + e_m$ .

### §9.6.2. Eliminating Shear Locking by RBF

How good is the nonlinear material stiffness (9.42)-(9.43)? If evaluated at the reference configuration aligned with the  $X$  axis,  $c_m = 1$ ,  $s_m = e_m = \gamma_m = 0$ , and we get

$$\mathbf{K}_M = \begin{bmatrix} \frac{EA_0}{L_0} & 0 & 0 & -\frac{EA_0}{L_0} & 0 & 0 \\ 0 & \frac{GA_0}{L_0} & \frac{1}{2}GA_0 & 0 & -\frac{GA_0}{L_0} & \frac{1}{2}GA_0 \\ 0 & \frac{1}{2}GA_0 & \frac{EI_0}{L_0} + \frac{1}{4}GA_0L_0 & 0 & -\frac{1}{2}GA_0 & -\frac{EI_0}{L_0} + \frac{1}{4}GA_0L_0 \\ -\frac{EA_0}{L_0} & 0 & 0 & \frac{EA_0}{L_0} & 0 & 0 \\ 0 & -\frac{GA_0}{L_0} & -\frac{1}{2}GA_0 & 0 & \frac{GA_0}{L_0} & -\frac{1}{2}GA_0 \\ 0 & \frac{1}{2}GA_0 & -\frac{EI_0}{L_0} + \frac{1}{4}GA_0L_0 & 0 & -\frac{1}{2}GA_0 & \frac{EI_0}{L_0} + \frac{1}{4}GA_0L_0 \end{bmatrix} \quad (9.44)$$

This is the well known *linear* stiffness of the  $C^0$  beam. As noted in the discussion of Section 9.2.4, this element does not perform as well as the  $C^1$  beam when the beam is thin because too

much strain energy is taken by shear. The following substitution device, introduced by MacNeal,<sup>7</sup> removes that deficiency in a simple way. The shear rigidity  $GA_0$  is formally replaced by  $12EI_0/L_0^2$ , and magically (9.44) becomes

$$\hat{\mathbf{K}}_M = \begin{bmatrix} \frac{EA_0}{L_0} & 0 & 0 & -\frac{EA_0}{L_0} & 0 & 0 \\ 0 & \frac{12EI_0}{L_0^3} & \frac{6EI_0}{L_0^2} & 0 & -\frac{12EI_0}{L_0^3} & \frac{6EI_0}{L_0^2} \\ 0 & \frac{6EI_0}{L_0^2} & \frac{4EI_0}{L_0} & 0 & -\frac{6EI_0}{L_0^2} & \frac{2EI_0}{L_0} \\ -\frac{EA_0}{L_0} & 0 & 0 & \frac{EA_0}{L_0} & 0 & 0 \\ 0 & -\frac{12EI_0}{L_0^3} & -\frac{6EI_0}{L_0^2} & 0 & \frac{12EI_0}{L_0^3} & -\frac{6EI_0}{L_0^2} \\ 0 & \frac{6EI_0}{L_0^2} & \frac{2EI_0}{L_0} & 0 & -\frac{6EI_0}{L_0^2} & \frac{4EI_0}{L_0} \end{bmatrix}. \quad (9.45)$$

This is the well known linear stiffness matrix of the  $C^1$  (Hermitian) beam based on the Euler-Bernoulli model. That substitution device is called the *residual bending flexibility* (RBF) correction.<sup>8</sup> Its effect is to get rid of the spurious shear energy due to the linear kinematic assumptions. If the RBF is formally applied to the nonlinear material stiffness one gets  $\hat{\mathbf{K}}_M = \mathbf{K}_M^a + \hat{\mathbf{K}}_{Mb}$ , where  $\mathbf{K}_M^a$  is the same as in (9.43) (because the axial stiffness is not affected by the substitution), whereas  $\mathbf{K}_M^b$  and  $\mathbf{K}_M^s$  merge into

$$\hat{\mathbf{K}}_M^b = \frac{EI}{L_0^3} \begin{bmatrix} 12s_m^2 & -12c_m s_m & 6a_1 L_0 s_m & -12s_m^2 & 12c_m s_m & 6a_1 L_0 s_m \\ -12c_m s_m & 12c_m^2 & -6c_m a_1 L_0 & 12c_m s_m & -12c_m^2 & -6c_m a_1 L_0 \\ 6a_1 L_0 s_m & -6c_m a_1 L_0 & a_2 L_0^2 & -6a_1 L_0 s_m & 6c_m a_1 L_0 & a_3 L_0^2 \\ -12s_m^2 & 12c_m s_m & -6a_1 L_0 s_m & 12s_m^2 & -12c_m s_m & -6a_1 L_0 s_m \\ 12c_m s_m & -12c_m^2 & 6c_m a_1 L_0 & -12c_m s_m & 12c_m^2 & 6c_m a_1 L_0 \\ 6a_1 L_0 s_m & -6c_m a_1 L_0 & a_3 L_0^2 & -6a_1 L_0 s_m & 6c_m a_1 L_0 & a_2 L_0^2 \end{bmatrix} \quad (9.46)$$

in which  $a_1 = 1 + e_m$ ,  $a_2 = 4 + 6e_m + 3e_m^2$  and  $a_3 = 2 + 6e_m + 3e_m^2$ .

**Remark 9.4.** MacNeal actually proposed the more refined substitution

$$\text{replace } \frac{1}{GA_0} \text{ by } \frac{1}{GA_s} + \frac{L_0^2}{12EI_0} \quad (9.47)$$

where  $GA_s$  is the *actual* shear rigidity; that is,  $A_s$  is the shear-reduced cross section studied in Mechanics of Materials. The result of (9.47) is the  $C^1$  Hermitian beam corrected by shear deformations computed from equilibrium considerations.<sup>9</sup> If the shear deformation is negligible, the right hand side of (9.47) is approximately  $L_0^2/(12EI_0)$ , which leads to the substitution used above.

<sup>7</sup> R. H. MacNeal, A simple quadrilateral shell element, *Computers and Structures*, **8**, 1978, pp. 175-183.

<sup>8</sup> RBF can be rigorously justified through the use of a mixed variational principle, or through a flexibility calculation.

<sup>9</sup> See, e.g., J. Przemieniecki, *Theory of Matrix Structural Analysis*, Dover, New York, 1968.

### §9.6.3. The Geometric Stiffness Matrix

The geometric stiffness  $\mathbf{K}_G$  comes from the variation of  $\mathbf{B}$  while the stress resultants in  $\mathbf{z}$  are kept fixed. To get a closed form expression it is convenient to pass to indicial notation, reverting to matrix notation later upon “index contraction.” Let the entries of  $\mathbf{K}_G$ ,  $\mathbf{B}$ ,  $\mathbf{u}$  and  $\mathbf{z}$  be denoted as  $K_{Gij}$ ,  $B_{ki}$ ,  $u_j$  and  $z_k$ , where indices  $i$ ,  $j$  and  $k$  range over 1–6, 1–6, and 1–3, respectively. Call  $\mathbf{A}^j = \partial\mathbf{B}/\partial u_j$ ,  $j = 1, \dots, 6$ . Then using the summation convention,

$$K_{Gij}\delta u_j = \int_{L_0} \delta\mathbf{B}^T \mathbf{z} dX = \int_{L_0} \frac{\partial B_{ki}}{\partial u_j} \delta u_j z_k dX = \int_{L_0} A_{ki}^j z_k dX \delta u_j, \quad (9.48)$$

whence

$$K_{Gij} = \int_{L_0} z_k A_{ki}^j d\bar{X}, \quad (9.49)$$

Note that in carrying out the derivatives in (9.49) by hand one must use the chain rule because  $\mathbf{B}$  is a function of  $e$ ,  $\gamma$  and  $\theta$ , which in turn are functions of the node displacements  $u_j$ . To implement this scheme we differentiate  $\mathbf{B}$  with respect to each node displacement in turn, to obtain:

$$\begin{aligned} \mathbf{A}^1 &= \frac{\partial\mathbf{B}}{\partial u_{x1}} = \frac{1}{L_0} \begin{bmatrix} 0 & 0 & \mathcal{N}_1 \sin \omega & 0 & 0 & \mathcal{N}_2 \sin \omega \\ 0 & 0 & \mathcal{N}_1 \cos \omega & 0 & 0 & \mathcal{N}_2 \cos \omega \\ 0 & 0 & 0 & 0 & 0 & 0 \end{bmatrix}, \\ \mathbf{A}^2 &= \frac{\partial\mathbf{B}}{\partial u_{y1}} = \frac{1}{L_0} \begin{bmatrix} 0 & 0 & -\mathcal{N}_1 \cos \omega & 0 & 0 & -\mathcal{N}_2 \cos \omega \\ 0 & 0 & \mathcal{N}_1 \sin \omega & 0 & 0 & \mathcal{N}_2 \sin \omega \\ 0 & 0 & 0 & 0 & 0 & 0 \end{bmatrix}, \\ \mathbf{A}^3 &= \frac{\partial\mathbf{B}}{\partial \theta_1} = \frac{\mathcal{N}_1}{L_0} \begin{bmatrix} \sin \omega & -\cos \omega & -\mathcal{N}_1 L_0(1+e) & -\sin \omega & \cos \omega & -\mathcal{N}_2 L_0(1+e) \\ \cos \omega & \sin \omega & -\mathcal{N}_1 L_0 \gamma & -\cos \omega & -\sin \omega & -\mathcal{N}_2 L_0 \gamma \\ 0 & 0 & 0 & 0 & 0 & 0 \end{bmatrix}, \\ \mathbf{A}^4 &= \frac{\partial\mathbf{B}}{\partial u_{x2}} = \frac{1}{L_0} \begin{bmatrix} 0 & 0 & -\mathcal{N}_1 \sin \omega & 0 & 0 & -\mathcal{N}_2 \sin \omega \\ 0 & 0 & -\mathcal{N}_1 \cos \omega & 0 & 0 & -\mathcal{N}_2 \cos \omega \\ 0 & 0 & 0 & 0 & 0 & 0 \end{bmatrix}, \\ \mathbf{A}^5 &= \frac{\partial\mathbf{B}}{\partial u_{y2}} = \frac{1}{L_0} \begin{bmatrix} 0 & 0 & \mathcal{N}_1 \cos \omega & 0 & 0 & \mathcal{N}_2 \cos \omega \\ 0 & 0 & -\mathcal{N}_1 \sin \omega & 0 & 0 & -\mathcal{N}_2 \sin \omega \\ 0 & 0 & 0 & 0 & 0 & 0 \end{bmatrix}, \\ \mathbf{A}^6 &= \frac{\partial\mathbf{B}}{\partial \theta_2} = \frac{\mathcal{N}_2}{L_0} \begin{bmatrix} \sin \omega & -\cos \omega & -\mathcal{N}_1 L_0(1+e) & -\sin \omega & \cos \omega & -\mathcal{N}_2 L_0(1+e) \\ \cos \omega & \sin \omega & -\mathcal{N}_1 L_0 \gamma & -\cos \omega & -\sin \omega & -\mathcal{N}_2 L_0 \gamma \\ 0 & 0 & 0 & 0 & 0 & 0 \end{bmatrix}. \end{aligned} \quad (9.50)$$

To restore matrix notation it is convenient to define

$$W_{Nij} = A_{1i}^j, \quad W_{Vij} = A_{2i}^j, \quad W_{Mij} = A_{3i}^j, \quad (9.51)$$

as the entries of three  $6 \times 6$  “weighting matrices”  $\mathbf{W}_N$ ,  $\mathbf{W}_V$  and  $\mathbf{W}_M$  that isolate the effect of the stress resultants  $z_1 = N$ ,  $z_2 = V$  and  $z_3 = M$ . The first, second and third row of each  $A^j$  becomes

the  $j^{\text{th}}$  column of  $\mathbf{W}_N$ ,  $\mathbf{W}_V$  and  $\mathbf{W}_M$ , respectively. The end result is

$$\mathbf{W}_N = \frac{1}{L_0} \begin{bmatrix} 0 & 0 & \mathcal{N}_1 \sin \omega & 0 & 0 & \mathcal{N}_2 \sin \omega \\ 0 & 0 & -\mathcal{N}_1 \cos \omega & 0 & 0 & -\mathcal{N}_2 \cos \omega \\ \mathcal{N}_1 \sin \omega & -\mathcal{N}_1 \cos \omega & -\mathcal{N}_1^2 L_0(1+e) & -\mathcal{N}_1 \sin \omega & \mathcal{N}_1 \cos \omega & -\mathcal{N}_1 \mathcal{N}_2 L_0(1+e) \\ 0 & 0 & -\mathcal{N}_1 \sin \omega & 0 & 0 & -\mathcal{N}_2 \sin \omega \\ 0 & 0 & \mathcal{N}_1 \cos \omega & 0 & 0 & \mathcal{N}_2 \cos \omega \\ \mathcal{N}_2 \sin \omega & -\mathcal{N}_2 \cos \omega & -\mathcal{N}_1 \mathcal{N}_2 L_0(1+e) & -\mathcal{N}_2 \sin \omega & \mathcal{N}_2 \cos \omega & -\mathcal{N}_2^2 L_0(1+e) \end{bmatrix} \quad (9.52)$$

$$\mathbf{W}_V = \frac{1}{L_0} \begin{bmatrix} 0 & 0 & \mathcal{N}_1 \cos \omega & 0 & 0 & \mathcal{N}_2 \cos \omega \\ 0 & 0 & \mathcal{N}_1 \sin \omega & 0 & 0 & \mathcal{N}_2 \sin \omega \\ \mathcal{N}_1 \cos \omega & \mathcal{N}_1 \sin \omega & -\mathcal{N}_1^2 L_0 \gamma & -\mathcal{N}_1 \cos \omega & -\mathcal{N}_1 \sin \omega & -\mathcal{N}_1 \mathcal{N}_2 L_0 \gamma \\ 0 & 0 & -\mathcal{N}_1 \cos \omega & 0 & 0 & -\mathcal{N}_2 \cos \omega \\ 0 & 0 & -\mathcal{N}_1 \sin \omega & 0 & 0 & -\mathcal{N}_2 \sin \omega \\ \mathcal{N}_2 \cos \omega & \mathcal{N}_2 \sin \omega & -\mathcal{N}_1 \mathcal{N}_2 L_0 \gamma & -\mathcal{N}_2 \cos \omega & -\mathcal{N}_2 \sin \omega & -\mathcal{N}_2^2 L_0 \gamma \end{bmatrix} \quad (9.53)$$

and  $\mathbf{W}_M = \mathbf{0}$ . Notice that the matrices must be symmetric, since  $\mathbf{K}_G$  derives from a potential. Then

$$\mathbf{K}_G = \int_{L_0} (\mathbf{W}_N N + \mathbf{W}_V V) d\bar{X} = \mathbf{K}_{GN} + \mathbf{K}_{GV}. \quad (9.54)$$

Again the length integral should be done with the one-point Gauss rule at  $\xi = 0$ . Denoting again quantities evaluated at  $\xi = 0$  by an  $m$  subscript, one obtains the closed form

$$\mathbf{K}_G = \frac{N_m}{2} \begin{bmatrix} 0 & 0 & s_m & 0 & 0 & s_m \\ 0 & 0 & -c_m & 0 & 0 & -c_m \\ s_m & -c_m & -\frac{1}{2}L_0(1+e_m) & -s_m & c_m & -\frac{1}{2}L_0(1+e_m) \\ 0 & 0 & -s_m & 0 & 0 & -s_m \\ 0 & 0 & c_m & 0 & 0 & c_m \\ s_m & -c_m & -\frac{1}{2}L_0(1+e_m) & -s_m & c_m & -\frac{1}{2}L_0(1+e_m) \end{bmatrix} \quad (9.55)$$

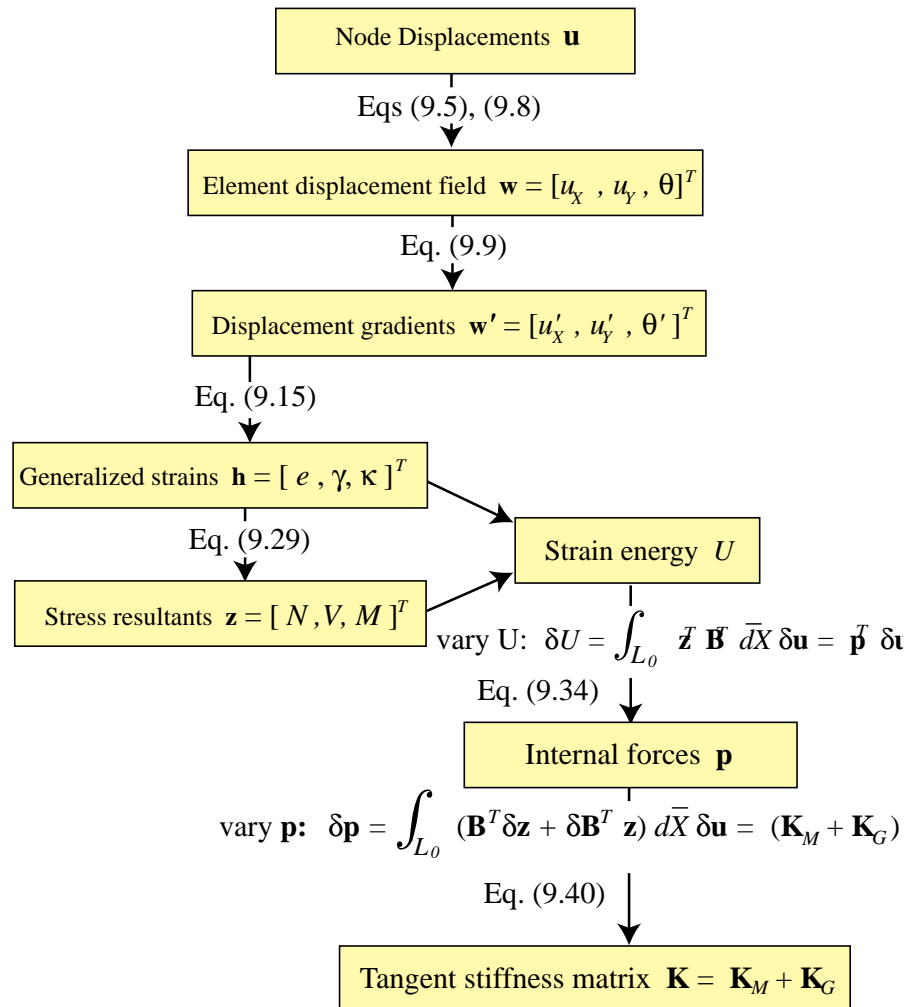
$$+ \frac{V_m}{2} \begin{bmatrix} 0 & 0 & c_m & 0 & 0 & c_m \\ 0 & 0 & s_m & 0 & 0 & s_m \\ c_m & s_m & -\frac{1}{2}L_0\gamma_m & -c_m & -s_m & -\frac{1}{2}L_0\gamma_m \\ 0 & 0 & -c_m & 0 & 0 & -c_m \\ 0 & 0 & -s_m & 0 & 0 & -s_m \\ c_m & s_m & -\frac{1}{2}L_0\gamma_m & -c_m & -s_m & -\frac{1}{2}L_0\gamma_m \end{bmatrix}.$$

in which  $N_m$  and  $V_m$  are  $N$  and  $V$  evaluated at the midpoint.

### §9.7. A Commentary on the Element Performance

The material stiffness of the present element works fairly well once MacNeal's RBF device is done. On the other hand, simple buckling test problems, as in Exercise 9.3, show that the geometric stiffness is not so good as that of the  $C^1$  Hermitian beam element.<sup>10</sup> Unfortunately a simple

<sup>10</sup> In the sense that one must use more elements to get equivalent accuracy.

Figure 9.10. Main steps in the derivation of the  $C^0$  plane beam element.

substitution device such as RBF cannot be used to improve  $\mathbf{K}_G$ , and the problem should be viewed as open.

An intrinsic limitation of the present element is the restriction to *small axial strains*. This was done to facilitate close form derivation. The restriction is adequate for many structural problems, particularly in Aerospace (example: deployment). However, it means that the element cannot model correctly problems like the snap-through and bifurcation of the arch example used in Chapter 8, in which large axial strains prior to collapse necessarily occur.

### §9.8. Summary

Figure 9.10 is a roadmap that summarizes the key steps in the derivation of the internal force and tangent stiffness matrix for the  $C^0$  plane beam element.

**Homework Exercises for Chapter 9**  
**The Plane Beam Element**

**EXERCISE 9.1** [A+N:20] Consider a plane prismatic beam of length  $L_0$ , cross section area  $A_0$  and second moment of inertia  $I_0$ . In the reference configuration the beam extends from node 1 at  $(X = Y = 0)$  to node 2 at  $(X = L_0, Y = 0)$ . The beam is under axial prestress force  $N^0 \neq 0$  in the reference configuration, while both  $V^0$  and  $M_0$  vanish.

- (a) Obtain the internal force  $\mathbf{p}$ , the material stiffness matrix  $\mathbf{K}_M$  and the geometric stiffness matrix  $\mathbf{K}_G$  in the reference configuration, for which  $u_{X1} = u_{Y1} = u_{X2} = u_{Y2} = \theta_1 = \theta_2 = 0$ .
- (b) The beam rotates  $90^\circ$  rigidly to a current configuration for which  $u_{X1} = u_{Y1} = 0, u_{X2} = -L_0, u_{Y2} = L_0, \theta_1 = \theta_2 = 90^\circ$ . Check that the stress resultants do not change (that is,  $N = N_0$  and  $V = M = 0$  because  $e = \gamma = \kappa = 0$ ), and obtain  $\mathbf{K}_M$  and  $\mathbf{K}_G$  in that configuration.

**EXERCISE 9.2**

[N:20] Analyze the pure bending of a cantilever discretized into an arbitrary number of elements.

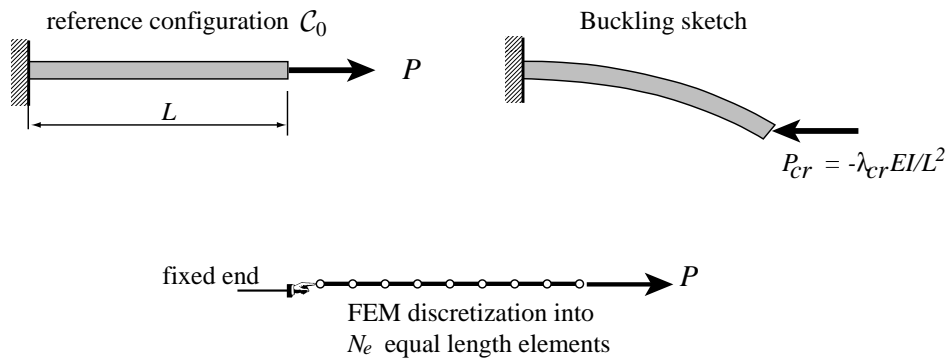


Figure E9.1. Structure for Exercises 9.3 and 9.4.

**EXERCISE 9.3**

[N:25] This exercise and the next one pertain to the simple structure shown in Figure E9.1. It is a cantilever, plane beam-column of length  $L$ , modulus  $E$ , area  $A$  and inertia  $I$ , loaded by an axial force  $P$  as shown. The structure is discretized into  $N_e$  plane beam elements of equal length. The structure moves in the plane of the figure. The objective is to compute the classical buckling load  $P_{cr}$  and compare with the known analytical value.

In the classical buckling analysis, deformations prior to buckling are neglected. The structure stiffness  $\mathbf{K} = \mathbf{K}_M + \mathbf{K}_G$  is evaluated on the reference configuration, with  $\mathbf{K}_G$  evaluated from the internal force state. This stability model is called *linearized prebuckling* or LPB, and is studied in detail in later Chapters. Under the LPB assumptions  $\mathbf{K}_M$  is constant while  $\mathbf{K}_G$  linear in the applied forces. Critical point analysis leads to a linear eigensystem called the buckling eigenproblem. The smallest eigenvalue characterizes the critical load, which for the LPB model can be shown to produce bifurcation.

The classical buckling load (also called Euler load) for the configuration of Figure E9.1 is  $P_{cr} = \lambda_{cr} EI / L^2$  with  $\lambda_{cr} = -\pi^2/4$  (negative because  $P$  has to compress the beam-column to achieve buckling). FEM results for  $N_e = 1, 2, \dots$  can be obtained by running the code of Figure A9.7. This script assembles  $\mathbf{K}$  taking in  ${}_0$  with  $E = I = A = L = 1$  to simplify computations while leaving  $P = \lambda$  symbolic. The only nonzero internal force is  $N_0 = P$ . The determinant  $\det(\mathbf{K})$  is formed explicitly as a polynomial in  $P$ , called the *characteristic polynomial*. All of its roots are computed via NSolve. The root closest to zero defines the critical load.

As answers to the exercise run the script until the largest  $N_e$  that can be reasonably handled by your *Mathematica* version (this will depend on memory and CPU speed). Termination can be controlled by adjusting the loop on  $k$ , which doubles  $N_e$  on each pass.

Report on the following items:

- (a) Your computed  $\lambda_{cr}$ 's for the  $N_e$  you were able to run. Comment on whether they converge toward  $-\pi^2/4$ . Is the convergence monotonic?
- (b) Why does `NSolve` give  $2N_e$  roots?<sup>11</sup>
- (c) Why are the roots real?<sup>12</sup>
- (d) Why do the computations get rapidly very slow as  $N_e$  increases?<sup>13</sup>

**EXERCISE 9.4** [N:20] The brute-force technique used to find  $\lambda_{cr}$  in Exercise 9.3 is easy to implement but it is extremely inefficient as the number of elements increase.<sup>14</sup>

A more effective technique is implemented in the script shown in Figure A9.8 of the Addendum. On *Mathematica* this works fine on my Mac up to 128 elements, beyond which point memory and CPU time requirements grow too large. As answer to this exercise:

- (a) Describe what is going on in the script.
- (b) Discuss why the solution is more efficient and robust than the previous script.<sup>15</sup>

---

<sup>11</sup> Only one of which is of practical interest.

<sup>12</sup> Assuming that exact integer arithmetic is used to form the determinant. If you form the determinant in floating-point complex roots will likely emerge because of numerical imprecision.

<sup>13</sup> If you can't guess, try printing the expanded determinant.

<sup>14</sup> Forming the characteristic polynomial by expanding  $\det(\mathbf{K})$  is frowned upon by numerical analysts for several reasons, one of which is that the polynomial coefficients tend to get enormously large. This requires either extended precision if done in integer arithmetic (as in the script) or rapidly lead to overflow if done in floating point.

<sup>15</sup> It is still far, however, from the optimal way to compute  $\lambda_{cr}$ . The practical technique used in production FEM codes is a variation on that script, using an eigensolution method called inverse power iteration.

## Addendum for Homework Exercises 9.3 and 9.4

The *Mathematica* Notebook `PlaneBeam.nb` contains several modules and scripts that support Exercises 9.3 and 9.4. The Notebook file is posted on the course Web site. The important pieces of code are briefly described in this Addendum.

Figure A9.1 shows module `FormIntForceCOTwoNodePlaneBeam`. This forms the internal force vector  $\mathbf{p}$  of a two-node,  $C^0$ , plane beam formulated with the TL description. Although this module is not directly called in Exercises 9.3 and 9.4, it is used later in the course. It is also used in the verification of the stiffness matrix modules by finite differences.

```
FormIntForceCOTwoNodePlaneBeam[XY1_,XY2_,u1_,u2_,S0_,z0_] :=Module[
  {X1,Y1,X21,Y21,L0,uX1,uY1,theta1,uX2,uY2,theta2,x21,y21,
   thetam,ctheta,stheta,Lcpsi,Lspsi,N0,V0,M0,EA0,GA0,EI0,
   cphi,sphi,cm,sm,Nm,Vm,Mm,kappa,p},
  {X1,Y1}=XY1; {X2,Y2}=XY2; X21=X2-X1; Y21=Y2-Y1;
  {uX1,uY1,theta1}=u1; {uX2,uY2,theta2}=u2;
  x21=X21+uX2-uX1; y21=Y21+uY2-uY1;
  L0=PowerExpand[Sqrt[X21^2+Y21^2]]; thetam=(theta1+theta2)/2;
  ctheta=Cos[thetam]; stheta=Sin[thetam];
  Lcpsi=Simplify[(X21*x21+Y21*y21)/L0];
  Lspsi=Simplify[(X21*y21-Y21*x21)/L0];
  em=(ctheta*Lcpsi+stheta*Lspsi)/L0-1;
  gm=-(stheta*Lcpsi-ctheta*Lspsi)/L0;
  kappa=(theta2-theta1)/L0;
  {N0,V0,M0}=z0; {EA0,GA0,EI0}=S0;
  Nm=Simplify[N0+EA0*em]; Vm=Simplify[V0+GA0*gm];
  Mm=Simplify[M0+EI0*kappa];
  cphi=X21/L0; sphi=Y21/L0;
  cm=ctheta*cphi-stheta*sphi; sm=stheta*cphi+ctheta*sphi;
  Bm=(1/L0)*{{-cm,-sm,L0*gm/2,cm,sm,L0*gm/2},
             {sm,-cm,-L0*(1+em)/2,-sm,cm,-L0*(1+em)/2},
             {0,0,-1,0,0,1}};
  p=L0*Transpose[Bm].{{Nm},{Vm},{Mm}};
  Return[Simplify[p]];

p=FormIntForceCOTwoNodePlaneBeam[{0,0},{L/Sqrt[2],L/Sqrt[2]},
  {0,0,Pi/2},{-2*L/Sqrt[2],0,Pi/2},
  {EA,GA0,EI},{0,V0,0}];
Print["p=",p];
```

Figure A9.1. Evaluation of internal force vector  $\mathbf{p}$  for plane beam element.

The 6 arguments of this module are  $XY1$ ,  $XY2$ ,  $u1$ ,  $u2$ ,  $S0$  and  $z0$ .  $XY1$  lists the coordinates  $\{X_1, Y_2\}$  of node 1 whereas  $XY2$  lists the coordinates  $\{X_1, Y_2\}$  of node 2, in the reference configuration.  $u1$  passes the three displacements:  $\{u_{X1}, u_{Y1}, \theta_1\}$  of node 1, and  $u2$  does the same for node 2.  $S0$  collects the section integrated constitutive properties  $\{EA_0, GA_0, EI_0\}$ . To apply MacNeal's RBF,  $GA_0$  should be replaced by  $12EI_0/L_0^2$  as discussed in Section 9.5. Finally  $z0$  passes the internal forces  $\{N_0, V_0, M_0\}$  in the reference configuration;

```

FormMatStiffCOTwoNodePlaneBeam[XY1_,XY2_,u1_,u2_,S0_,z0_] :=
Module[{X1,Y1,X21,Y21,L0,uX1,uY1,theta1,uX2,uY2,theta2,x21,y21,
  thetam,ctheta,stheta,Lcpsi,Lspsi,N0,V0,M0,EA0,GA0,EI0,
  cphi,sphi,cm,sm,a1,KM},
{X1,Y1}=XY1; {X2,Y2}=XY2; X21=X2-X1; Y21=Y2-Y1;
{uX1,uY1,theta1}=u1; {uX2,uY2,theta2}=u2;
x21=X21+uX2-uX1; y21=Y21+uY2-uY1;
L0=PowerExpand[Sqrt[X21^2+Y21^2]]; thetam=(theta1+theta2)/2;
ctheta=Cos[thetam]; stheta=Sin[thetam];
Lcpsi=Simplify[(X21*x21+Y21*y21)/L0];
Lspsi=Simplify[(X21*y21-Y21*x21)/L0];
em=(ctheta*Lcpsi+stheta*Lspsi)/L0-1;
gm=-(stheta*Lcpsi-ctheta*Lspsi)/L0;
cphi=X21/L0; sphi=Y21/L0;
cm=ctheta*cphi-stheta*sphi; sm=stheta*cphi+ctheta*sphi;
{N0,V0,M0}=z0; {EA0,GA0,EI0}=S0; a1=1+em;
KM = (EA0/L0)*{
{ cm^2,cm*sm,-cm*gm*L0/2,-cm^2,-cm*sm,-cm*gm*L0/2},
{ cm*sm,sm^2,-gm*L0*sm/2,-cm*sm,-sm^2,-gm*L0*sm/2},
{-cm*gm*L0/2,-gm*L0*sm/2,gm^2*L0^2/4,
  cm*gm*L0/2,gm*L0*sm/2,gm^2*L0^2/4},
{-cm^2,-cm*sm,cm*gm*L0/2,cm^2,cm*sm,cm*gm*L0/2},
{-cm*sm,-sm^2,gm*L0*sm/2,cm*sm,sm^2,gm*L0*sm/2},
{-cm*gm*L0/2,-gm*L0*sm/2,gm^2*L0^2/4,
  cm*gm*L0/2,gm*L0*sm/2,gm^2*L0^2/4}}+
(EI0/L0)*{{0,0,0,0,0,0}, {0,0,0,0,0,0},
{0,0,1,0,0,-1}, {0,0,0,0,0,0},
{0,0,0,0,0,0}, {0,0,-1,0,0,1}}+
(GA0/L0)*{
{sm^2,-cm*sm,-a1*L0*sm/2,-sm^2,cm*sm,-a1*L0*sm/2},
{-cm*sm,cm^2,cm*a1*L0/2,cm*sm,-cm^2,cm*a1*L0/2},
{-a1*L0*sm/2,cm*a1*L0/2, a1^2*L0^2/4,
  a1*L0*sm/2,-cm*a1*L0/2, a1^2 L0^2/4},
{-sm^2,cm*sm, a1*L0*sm/2,sm^2,-cm*sm,a1*L0*sm/2},
{ cm*sm,-cm^2,-cm*a1*L0/2,-cm*sm,cm^2,-cm*a1*L0/2},
{-a1*L0*sm/2,cm*a1*L0/2,a1^2*L0^2/4,
  a1*L0*sm/2,-cm*a1*L0/2, a1^2*L0^2/4}};
Return[KM ]];

```

Figure A9.2. Evaluation of material stiffness matrix  $\mathbf{K}_M$  for plane beam element.

these forces are assumed to be constant along the element. Thmodule forms the internal force vector  $\mathbf{p}$  with a one point integration rule as discussed earlier, and returns  $\mathbf{p}$  as function value.

Figures A9.2 and A9.3 show modules FormMatStiffCOTwoNodePlaneBeam and FormGeoStiffCOTwoNodePlaneBeam. As their name suggest, these form the material and geometric stiffness components, respectively, of the plane beam element. They have been separated for convenience although for most applications they are combined to form the tangent stiffness matrix. The 6 arguments are exactly the

```

FormGeoStiffCOTwoNodePlaneBeam[XY1_,XY2_,u1_,u2_,S0_,z0_] :=
Module[{X1,Y1,X21,Y21,L0,uX1,uY1,theta1,uX2,uY2,theta2,
  x21,y21,thetam,ctheta,stheta,Lcpsi,Lspsi,
  N0,V0,M0,EA0,GA0,EI0,cphi,sphi,cm,sm,Nm,Vm,KG},
  {X1,Y1}=XY1; {X2,Y2}=XY2; X21=X2-X1; Y21=Y2-Y1;
  {uX1,uY1,theta1}=u1; {uX2,uY2,theta2}=u2;
  x21=X21+uX2-uX1; y21=Y21+uY2-uY1;
  L0=PowerExpand[Sqrt[X21^2+Y21^2]]; thetam=(theta1+theta2)/2;
  ctheta=Cos[thetam]; stheta=Sin[thetam];
  Lcpsi=Simplify[(X21*x21+Y21*y21)/L0];
  Lspsi=Simplify[(X21*y21-Y21*x21)/L0];
  em=(ctheta*Lcpsi+stheta*Lspsi)/L0-1;
  gm=-(stheta*Lcpsi-ctheta*Lspsi)/L0;
  kappa=(theta2-theta1)/L0;
  {N0,V0,M0}=z0; {EA0,GA0,EI0}=S0;
  Nm=Simplify[N0+EA0*em]; Vm=Simplify[V0+GA0*gm];
  cphi=X21/L0; sphi=Y21/L0;
  cm=ctheta*cphi-stheta*sphi; sm=stheta*cphi+ctheta*sphi;
  KG = Nm/2*{{0, 0, sm, 0, 0, sm}, {0, 0, -cm, 0, 0,-cm},
    {sm, -cm, -(L0/2)*(1+em), -sm, cm,-(L0/2)*(1+em)},
    {0, 0, -sm, 0, 0, -sm}, {0, 0, cm, 0, 0, cm},
    {sm, -cm, -(L0/2)*(1+em), -sm, cm,-(L0/2)*(1+em)}}+
  Vm/2*{{0, 0, cm, 0, 0, cm}, {0, 0, sm, 0, 0, sm},
    {cm, sm, -(L0/2)*gm, -cm, -sm,-(L0/2)*gm},
    {0, 0, -cm, 0, 0, -cm}, {0, 0, -sm, 0, 0, -sm},
    {cm, sm, -(L0/2)*gm, -cm, -sm,-(L0/2)*gm}};
  Return[KG] ];

```

Figure A9.3. Evaluation of geometric stiffness matrix  $\mathbf{K}_G$  for plane beam element.

```

FormTanStiffCOTwoNodePlaneBeam[XY1_,XY2_,u1_,u2_,S0_,z0_] :=
Module[{},
  KM=FormMatStiffCOTwoNodePlaneBeam[XY1,XY2,u1,u2,S0,z0];
  KG=FormGeoStiffCOTwoNodePlaneBeam[XY1,XY2,u1,u2,S0,z0];
  Return[KM+KG]];

ClearAll[EA,GA,EI];
KM=FormMatStiffCOTwoNodePlaneBeam[{0,0},{10,0},{0,0,0},{0,0,0},
  {EA,GA,EI},{0,0,0}]; Print[KM];
KG=FormGeoStiffCOTwoNodePlaneBeam[{0,0},{4,3},{0,0,0},{0,0,0},
  {1,1,1},{10,30,20}]; Print[KG];
Print[Chop[Eigenvalues[N[KG]]]];

```

Figure A9.4. Evaluation of tangent stiffness matrix  $\mathbf{K}$  for plane beam element, along with test statements.

```

MergeElemIntoMasterIntForce[pe_,eftab_,pm_] :=
  Module[{i,ii,nf=Length[eftab],p}, p=pm;
    For[i=1, i<=nf, i++, ii=eftab[[i]];
      If [ii>0,p[[ii,1]]+=pe[[i,1]]]
    ]; Return[p]
];

MergeElemIntoMasterStiff[Ke_,eftab_,Km_] :=
  Module[{i,j,ii,jj,nf=Length[eftab],K}, K=Km;
    For[i=1, i<=nf, i++, ii=eftab[[i]]; If[ii==0,Continue[]];
      For[j=i, j<=nf, j++, jj=eftab[[j]];
        If [ii>0 && jj>0,
          K[[jj,ii]]=K[[ii,jj]]+=Ke[[i,j]]]
        ]
      ]; Return[K]
];

```

Figure A9.5. Merge modules for master internal force and master stiffness of a plane beam structure.

same as for the internal force module, Both matrices are formed with the one-point integration rule and are return as function values. The correctness of the implementation is checked with a finite difference technique implemented in a script not listed here.

Figure A9.4 lists module `FormTanStiffCOTwoNodePlaneBeam`, which returns the tangent stiffness matrix  $\mathbf{K} = \mathbf{K}_M + \mathbf{K}_G$ . It simple calls the previous two modules and returns the matrix sum as function value.

Figure A9.5 lists two modules that merge the internal force vector and stiffness matrix, respectively, of one individual element into the corresponding master quantities for the entire structure.

Figure A9.6 lists two modules: `AssembleMasterStiffOfCantBeam` and `AssembleMasterIntForceOfCantBeam` that assemble  $\mathbf{p}$  and  $\mathbf{K}$ , respectively, for one specific structure. This structure is the cantilever beam-column under axial force  $P$  shown in Figure E9.1, discretized into  $N_e \geq 1$  plane beam elements.

Figures A9.7 and A9.8 lists two scripts for use in Exercises 9.3 and 9.4, respectively.

```

AssembleMasterIntForceOfCantBeam[{L_, P_, Ne_}, {Em_, A0_, I0_}, u_] :=
Module[{e, numnod, numdof, u1, u2, u3, Le, X1, X2, S0, z0, eftab,
  pe, p},
  numnod=Ne+1; numdof=3*numnod; Le=L/Ne;
  p=Table[0, {numdof}, {1}];
  z0={P, 0, 0}; S0={Em*A0, 12*Em*I0/Le^2, Em*I0}; (* RBF *)
  For [e=1, e<=Ne, e++,
    X1=(e-1)*Le; X2=e*Le;
    If [e==1, u1={0, 0, 0}; u2=Take[u, {3*e-2, 3*e}];
      eftab={0, 0, 0, 3*e-2, 3*e-1, 3*e}];
    If [e>1, u1=Take[u, {3*e-5, 3*e-3}]; u2=Take[u, {3*e-2, 3*e}];
      eftab={3*e-5, 3*e-4, 3*e-3, 3*e-2, 3*e-1, 3*e}];
    pe=FormIntForceCOTwoNodePlaneBeam[{X1, 0}, {X2, 0}, u1, u2, S0, z0];
    (*Print["pe=", pe];*)
    p=MergeElemIntoMasterIntForce[pe, eftab, p];
  ];
  Return[Simplify[p]]
];

AssembleMasterStiffOfCantBeam[{L_, P_, Ne_}, {Em_, A0_, I0_}, u_] :=
Module[{e, numnod, numdof, u1, u2, u3, Le, X1, X2, S0, z0, eftab,
  pe, p},
  numnod=Ne+1; numdof=3*numnod-3; Le=L/Ne;
  K=Table[0, {numdof}, {numdof}];
  z0={P, 0, 0}; S0={Em*A0, 12*Em*I0/Le^2, Em*I0}; (* RBF *)
  For [e=1, e<=Ne, e++,
    X1=(e-1)*Le; X2=e*Le;
    If [e==1, u1={0, 0, 0}; u2=Take[u, {3*e-2, 3*e}];
      eftab={0, 0, 0, 3*e-2, 3*e-1, 3*e}];
    If [e>1, u1=Take[u, {3*e-5, 3*e-3}]; u2=Take[u, {3*e-2, 3*e}];
      eftab={3*e-5, 3*e-4, 3*e-3, 3*e-2, 3*e-1, 3*e}];
    Ke=FormTanStiffCOTwoNodePlaneBeam[{X1, 0}, {X2, 0}, u1, u2, S0, z0];
    (*Print["Ke=", Ke];*)
    K=MergeElemIntoMasterStiff[Ke, eftab, K];
  ];
  Return[Simplify[K]]
];

```

Figure A9.6. Assembly modules for cantilevered beam-column under axial load.

```

ClearAll[L,P,Em,A0,I0]; Em=A0=I0=L=1; Ne=1;
For [k=1, k<=6, k++,
  Print["Number of elements=",Ne];
  LPNe={L,P,Ne}; EAI={Em,A0,I0}; u=Table[0,{3*Ne+3}];
  K=AssembleMasterStiffOfCantBeam[LPNe,EAI,u];
  (*Print["K=",K//MatrixForm];*)
  detK=Det[K];
  (*Print["det(K)=",detK//InputForm];*)
  roots=NSolve[detK==0,P];
  Print["roots of stability det=",roots]; Ne=2*Ne;
];
Print["exact buckling load coeff is ",-N[Pi^2/4]];

```

Figure A9.7. Script for Exercise 9.3. It uses assembly, merge and element formation modules.

```

ClearAll[L,P,Em,A0,I0]; Em=A0=I0=L=1; Ne=1;
For [k=1, k<=8, k++,
  Print["Number of elements=",Ne];
  LPNe={L,P,Ne}; EAI={Em,A0,I0}; u=Table[0,{3*Ne+3}];
  K=AssembleMasterStiffOfCantBeam[LPNe,EAI,u];
  KM=Coefficient[K,P,0]; KG=Coefficient[K,P,1];
  SG=LinearSolve[N[KM],N[KG]];
  (*Print["KM=",KM//MatrixForm]; Print["KG=",KG//MatrixForm];*)
  (*Print["SG=",SG//MatrixForm];*)
  emax=-Max[Eigenvalues[SG]]; Print["FEM lambda cr=",1/emax];
  Ne=2*Ne;
];
Print["exact buckling lambda coeff is ",-N[Pi^2/4]//InputForm];

```

Figure A9.8. Script for Exercise 9.4. It uses assembly, merge and element formation modules.